Journal of Hazardous Materials 473 (2024) 134716

Contents lists available at ScienceDirect

Journal of Hazardous Materials

journal homepage: www.elsevier.com/locate/jhazmat

Two different types of hydrolases co-degrade ochratoxin A in a highly efficient degradation strain *Lysobacter* sp. CW239

Xiaojie Fu [a], Qingru Fei [a], Xuanjun Zhang [a], Na Li [a], Liang Zhang [b], Yu Zhou [a,b,c,*]

[a] State Key Laboratory of Tea Plant Biology and Utilization, Anhui Agricultural University, Heifei 230036, China
[b] School of Tea and Food Science Technology, Anhui Agricultural University, Heifei 230036, China
[c] Joint Research Center for Food Nutrition and Health of IHM, Hefei 230036, China

HIGHLIGHTS

- Carboxypeptidase CP4 and amidohydrolase ADH2 co-degraded OTA in strain CW239.
- Amidohydrolase ADH2 was the overwhelming efficient detoxify enzyme in strain CW239.
- Hydrolases CP4 and ADH2 co-degraded OTA in strain CW239 by synergistic effect.
- Degradation mechanism of strain CW239 was validated by in vitro and in vivo methods.

GRAPHICAL ABSTRACT

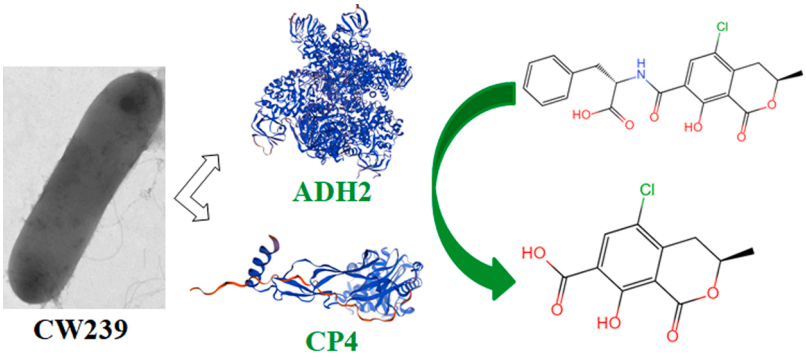

ARTICLE INFO

Keywords:
Ochratoxin A
Detoxification
Contamination
Amidohydrolase
Carboxypeptidase

ABSTRACT

Ochratoxin A (OTA) is a toxic secondary metabolite that widely contaminates agro-products and poses a significant dietary risk to human health. Previously, a carboxypeptidase CP4 was characterized for OTA degradation in *Lysobacter* sp. CW239, but the degradation activity was much lower than its host strain CW239. In this study, an amidohydrolase ADH2 was screened for OTA hydrolysis in this strain. The result showed that 50 μg/L OTA was completely degraded by 1.0 μg/mL rADH2 within 5 min, indicating ultra-efficient activity. Meanwhile, the two hydrolases (i.e., CP4 and ADH2) in the strain CW239 showed the same degradation manner, which transformed the OTA to ochratoxin α (OTα) and L-*β*-phenylalanine. Gene mutants (Δ*cp4*, Δ*adh2* and Δ*cp4-adh2*) testing result showed that OTA was co-degraded by carboxypeptidase CP4 and amidohydrolase ADH2, and the two hydrolases are sole agents in strain CW239 for OTA degradation. Hereinto, the ADH2 was the overwhelming efficient hydrolase, and the two types of hydrolases co-degraded OTA in CW239 by synergistic effect. The results of this study are highly significant to ochratoxin A contamination control during agro-products production and postharvest.

* Corresponding author at: State Key Laboratory of Tea Plant Biology and Utilization, Anhui Agricultural University, Heifei 230036, China.
E-mail address: microbes@ahau.edu.cn (Y. Zhou).

https://doi.org/10.1016/j.jhazmat.2024.134716
Received 13 February 2024; Received in revised form 6 May 2024; Accepted 22 May 2024
Available online 23 May 2024
0304-3894/© 2024 Elsevier B.V. All rights are reserved, including those for text and data mining, AI training, and similar technologies.

1. Introduction

Mycotoxins are toxic secondary metabolites of filamentous fungi, which are known to contaminate a wide range of agro-products (e.g., cereals, oils, fruits, nuts and their processed foods), resulting in harmful effects to humans and animals [1]. To date, more than 400 mycotoxins have been identified; ochratoxin is one of the most important group, not only due to its potential toxicity, but also because it is heavily contamination, resulting in widespread exposure [2–4]. Ochratoxin belongs to the group of isocoumarin-derived compound linked to L-β-phenylalanine in the chemical structure, and mainly produced by toxigenic strains of *Aspergillus* spp. and *Penicillium* spp.; hereinto, ochratoxin A (OTA) is most toxic and widely contaminated ochratoxin for agro-products [5]. Grapes, cacao, coffee, oats, barley, wheat and corn are the most susceptible agricultural products to OTA contamination, and the contaminations can pose health risks in human and livestocks [6]. OTA detoxification methods showed high interest in contamination control in foodstuff and agricultural production [7,8]. Due to the merits of environmental friendly, specific and high efficiency, biodegradation has emerged as a prominent research topic among various methods for mycotoxin detoxification, including OTA [9,10].

Generally, two methods of detoxification, including bioadsorption and biodegradation have been extensively studied for microbial strains. For example, *Saccharomyces* spp., *Lactobacillus* spp. and *Bacillus* spp. can remove OTA effectively by cell adsorption [11,12]. At the same time, other microbial strains can degrade or transforme OTA to other nontoxic (or less toxic) products by active enzymes, such as carboxypeptidase, amidase, ochratoxinase, amidohydrolase and lipase [13,14]. The study of Zhang et al. showed that OTA was transformed to OTα by carboxypeptidase in *Yarrowia lipolytica* through amido bond hydrolyzation [15]. Cho et al. showed that *Aspergillus tubingensis* degraded OTA through bioenzyme, the crude enzyme prepared from *A. tubingensis* culture removed more than 90 % OTA at pH of 5.0, but the active protein was not purified [16]. Ochratoxinase (OTase) which was firstly characterized as amidase from *Aspergillus niger* showed much higher efficient activity than those of carboxypeptidases A (CPA) and carboxypeptidase Y (CPY). In addition, OTase was the first protein crystal structure unveiled OTA detoxify enzyme, which is of great significance in understanding of the hydrolytic mechanism for this kind of hydrolase [17]. Garcia et al. found that OTA could be degraded by commercial peroxidase in buffer solution and beer [18]. Currently, several types of hydrolases were characterized for OTA degradation [19–24]. Hereinto, amidohydrolase was the most focused OTA detoxify enzyme in last two years, such as amidohydrolase *Af*OTase from *Alcaligenes faecalis* [25], ADH3 and NA from *Stenotrophomonas acidaminiphila* [24,26], *Bn*OTAase4 from *Brevundimonas naejangsanensis* [19] and *Ps*SDO from *Pseudaminobacter salicylatoxidans* [23]. Meanwhile, the OTase that previously assigned as amidase also belongs to amidohydrolase family based on amino acids sequence analysis result [24,26].

In previous study, we found that *Lysobacter* sp. CW239 that isolated from a polycyclic aromatic hydrocarbons (PAHs) contaminated soil sample showed efficient degradation activity to OTA, but the carboxypeptidase rCP4 that screened from the strain CW239 showed very limited OTA degradation activity [27]. Meanwhile, when the gene *cp4* was knockout from the host strain CW239, the mutant Δ*cp4* showed only 10 % recuction of OTA degradation activity [28]. These results suggested that other more efficient detoxify enzyme(s) might present in the strain CW239. Additionally, it appears that the OTA degradation in strain CW239 should be a result of the combined actions of multiple enzymes [28]. In this study, other OTA degrdation genes were screened and characterized, and the combined effect on OTA degradation was verified by in vivo and in vitro methods.

2. Materials and methods

2.1. Materials

Strains, plasmids and PCR primers used in this study are shown in Table 1. Wild-type strain *Lysobacter* sp. CW239 and gene *cp4* mutant (Δ*cp4*) were isolated or constructed previously in our laboratory [27,28], Gene mutants of Δ*adh2* and Δ*cp4-adh2*, and gene complementary strains of (Δ*cp4-adh2*)/*adh2* and (Δ*cp4-adh2*)/*cp4* were constructed in this study. *Escherichia coli* (*E. coli*) Trans1-T1, *E. coli* BL21 and *E. coli* BL21 (DE3) were purchased from TransGen Biotech (Beijing China). Microbial culture media, such as nutrient agar, nutrient broth and Luria-Bertani (LB) were the products of Hopebio (Qingdao, China). OTA standard (≥98.0 % purity) was purchased from Pribolab (Qingdao, China). Chromatographic grade (≥99.99 % purity) of methanol, acetonitrile and acetic acid were the products of TEDIA (Shanghai, China). Restriction endonucleases, DNA ligase and other commercial enzymes were the products of Takara (Dalian, China). PCR primers, antibiotics (i.e., Kanamycin, Ampicillin and Gentamycin) and other chemical reagents (≥98.0 % purity) were purchased from Sangon Biotech (Shanghai, China).

2.2. Genome analysis and potential detoxify enzymes screening

Genomic DNA of the strain CW239 was extracted and purified by a DNA isolation kit (Qiagen, Shanghai China) according to the manufacturer's instruction. Genome sequencing was commissioned to MAGIGENE Biotechnology Co., Ltd (Guangzhou, China) using the sequencing platforms of Novaseq 6000 sequencer and PacBio Sequel II. Clean reads from PacBio Sequel II were assembled by SMRT Link v5.1.0. Putative open reading frames (ORFs) were identified by Prodigal [29] or Glimmer 3.02 [30]. Gene annotation was performed by BLAST search in corresponding databases, including, the COG (Clusters of Orthologous Groups) [31], NR (Non-redundant Proteins) [32], GO (Gene Ontology) [33], KEGG (Kyoto Encyclopedia of Genes and Genomes) [34], Pfam [35], Swiss-prot [36], CAZy (Carbohydrate-Active Enzymes Database) [37], PHI (Pathogen Host Interactions) [38], VFDB (Virulence Factors of Pathogenic Pacteria) [39], and ARDB (Antibiotic Resistance Genes Database) [40]. Based on the gene annotation, the genes encoding carboxypeptidase, amidase and amidohydrolase that are possible candidates for OTA detoxification were screened out for the following protein expression and OTA degradation test by in vitro method.

2.3. Gene cloning, heterologous expression and protein purification

The genes of OTA degradation candidate were amplified using the gDNA of CW239 and specific primers for each gene (Table S4). PCR amplifications were carried out with Primerstar max DNA polymerase (TaKaRa, Dalian China). The purified PCR product (e.g., gene *adh2*) and expression plasmid (pMAL-c2X or pET-28a) were digested by *Xba*I (or other corresponding endonuclease) and *Hind* III (or other corresponding endonuclease), respectively. The digested PCR product and plasmid were ligated by the Solution I (TaKaRa, Dalian China) at 16 °C for 1 h, and transformed into competence cells of *E. coli* Trans1-T1 [24]. The transformed cells were clutured on LB agar with 50 μg/mL ampicillin (AmpR), and the clones were verified by PCR. The correct transformant was enriched with LB broth (AmpR), and the recombinant plasmid (e.g., pMAL-c2X/*adh2*) was extracted, verified and transformed into *E.coli* BL21 (DE3). The *E. coli* BL21 (DE3) transformant was cultured in LB medium (AmpR) at 37 ℃. Until optical density (OD_{600}) of the bacterial culture reached about 0.6, protein expression was induced by 0.1 mM isopropyl-β-D-thiogalactoside (IPTG) at 16 ℃ for 20 h. After protein expression, 30 mL bacterial cells were collected by centrifugation at 9000 ×*g* for 10 min, the bacterial cells were washed twice with 10 mL washing buffer (20 mmol/L Tris-HCl, 200 mmol/L NaCl, 1 mmol/L EDTA and 1 mmol/L DTT, pH 7.2). The washed cells were resuspended

Table 1
Bacterial strains, plasmids and the PCR primers used in this study.

Strain, plasmid or PCR primer	Characterization	Reference/ restriction sites
CW239	Wild-type degradation strain	[27]
Δ*cp4*	Gene *cp4* mutant of CW239	[28]
Δ*adh2*	Gene *adh2* mutant of CW239	this study
Δ*cp4-adh2*	Double gene (*cp4* and *adh2*) mutant of CW239	this study
(Δ*cp4-adh2)/adh2*	Gene *adh2* complementary for Δ*cp4-adh2* (GmR)	this study
(Δ*cp4-adh2)/cp4*	Gene *cp4* complementary for Δ*cp4-adh2* (GmR)	this study
BL21	Gene expression host	TransGen Biotech
BL21 (DE3)	Gene expression host	TransGen Biotech
pK18*mobsacB*	Allelic exchange vector (KmR)	[26]
pSRKGm	Gene complementary vector (GmR)	[26]
pMAL-c2X	Gene expression vector (AmpR)	Sangon Biotech
pET-28a	Gene expression vector (KmR)	Sangon Biotech
adh2-F	GCTCTAGAATGACCGTCCGCCTGG	*Xba* I
adh2-R	CCCAAGCTTTCATGGCGACGTCCCG	*Hind* III
adh2-US-F	GCTCTAGACGGTTCGGCCAGCAAGG	*Xba* I
adh2-US-R	ATGACGCCCCCGCTCGC	
adh2-DS-F	*GGGGCGAGCGGGGGCGTCAT*TCATTCAGGCCGCGCG	
adh2-DS-R	CCCAAGCTTGCAGCCACCTCCACATC	*Hind* III
ver-F	AACTGCCGTGGTATTCG	
ver-R	ACCGGGCAACGTCTATT	
com-*adh2*-F	GGAATTCCATATGATGACCGT CCGCCTGG	*Nde* I
com-*adh2*-R	CTAGCTAGCTCATGGCGACGTCCCG	*Nhe* I
com-*cp4*-F	GGAATTCCATATGATGAAGTCTCCCGCCG	*Nde* I
com-*cp4*-R	CTAGCTAGCTCAGGCCGACTGCCAC	*Nhe* I
F_{adh2}	CAAATCCATCGCCACCACC	
R_{adh2}	CGTCGCTGCCGTCTTTGTAC	
F_{gapdh}	TCCTGCGTTCTGCGATTCA	
R_{gapdh}	GGTCAGGCGGATCTTCTTGC	

The underlined sequence in PCR primer indicates the restriction site for endonuclease. KmR, kanamycin resistance; AmpR, ampicillin resistance; GmR, gentamicin resistance.

in 15 mL washing buffer, disintegrated by an ultrasonicator (Qsonica Q700, CT, USA), and crude enzyme (i.e., supernatant) was collected by centrifugation at 12,000 ×*g* for 10 min. Gene expression result (crude enzyme) was examined by Sodium Dodecyl Sulphate-PolyAcrylamide Gel Electrophoresis (SDS-PAGE; Bio-Rad, Hercules, USA) according to the standard protocol.

OTA degradation was determined by 0.5 mL crude enzyme and 0.5 mL OTA standard (80 μg/mL) that prepared by phosphate buffer solution (PBS, pH 7.2) at 37 ℃ for 12 h. The crude enzyme with degradation activity was purified by affinity chromatography with Amylose Resin (BioLabs, USA) or other corresponding affinity Resin according to the manufacturer's instruction. The purified recombinant enzymes (e.g., rADH2) were examined by SDS-PAGE, and the protein content was determined by spectrophotometrically method with BSA (bovine serum albumin) as the protein standard [41].

2.4. Sequence analysis of detoxify enzyme ADH2

Predictions of signal peptides (SP), molecular weight (*Mw*) and theoretical isoelectric point (pI) were performed by using online programs SignalP 6.0 and ExPASy [42,43]. Sequence similarity comparison to other closely related detoxify enzymes were analyzed by BLASTP (http://www.ncbi.nlm.nih.gov). The complete protein sequences of the related detoxify enzymes that retrieved from the GenBank database were multiple aligned for conserved regions and catalytic sites (i.e., active sites) analysis by using the CLUSTAL_X software [17,24].

2.5. Enzymatic characterization of rADH2

For temperature evaluation, a total of 300 μL degradation solution containing 10 μL active protein (30 μg/mL) and 290 μL of PBS diluted OTA standard (40 μg/L) was prepared, the degradation tubes were incubated at 20 − 90 ℃ for 2 min with the temperature interval of 10 ℃ of each treatment. The optimal pH was assayed by the method of Luo et al., the pH range from 3.0- 11.0 with the interval of 1.0 was determined [24], and the degradation was performed at 40 ℃ for 2 min. In protein denaturant and protease resistant assays, rADH2 was first pretreated with 1.0 % SDS, 1.0 mg/mL protease K or 1.0 % SDS plus 1.0 mg/mL protease K before the OTA degradation test. The pretreatment was performed at 40 ℃ for 6 h. OTA degradation was evaluated by 5 μL pretreated rADH2 solution and 295 μL PBS diluted OTA standard (40 μg/L, pH 7.2) at 40 ℃ for 3 min. The denaturant (1.0 % SDS or 1.0 mg/mL protease K) and the untreated rADH2 were selected as negative and positive controls, respectively. In metal-chelator assay, rADH2 was pretreated by 0.1 mol/L ethylene diamine tetraacetic acid (EDTA) or ethylene glycol-bis (beta-aminoethyl ether)-N-tetraacetic acid (EGTA) at 40 °C for 6 h. OTA degradation was determined by 5 μL metal-chelator pretreated rADH2 and 295 μL PBS diluted OTA standard (40 μg/L) at 40 ℃ for 3 min. The EDTA (or EGTA) solution and the untreated rADH2 were selected as negative and positive controls, respectively. Metal ions effect on rADH2 was evaluated by adding 0.01 mol/L (final concentration) Li^+, Mg^{2+}, Zn^{2+}, Fe^{2+}, Ni^{2+}, Ca^{2+}, Cu^{2+} or Mn^{2+} in 300 μL degradation solution and incubated at 40 ℃ for 3 min. Moreover, Li^+ effect on rADH2 was further evaluated by the final concentrations of 0.01, 0.05, 0.10 and 0.20 mol/L, respectively. After degradation tests, the residual OTA was detected by high performance liquid chromatography (HPLC) following the method as Wei et al. [27].

2.6. Kinetic constant assay

Serial concentrations of OTA standard (10 −90 μg/L) were prepared by PBS (pH 7.2) with the interval of 10 μg/L. The enzymatic reaction for each OTA concentration was performed by 5.0 μL of purified enzyme and 295 μL of OTA standard at 40 ℃ for appropriate time. Herein, the protein concentration of rADH2 was 1.0 μg/mL, and the protein concentration of rCP4 was 1.0 mg/mL; the incubation time for rADH2 was 3 min, and the incubation time for rCP4 was 24 h. The catalysate of OTα was cleaned and collected using the OchraTest column (Vicam, Milford, MA, USA), and then determined by HPLC. The reaction rates versus the substrate concentrations were plotted, and kinetic constants (K_{cat}, K_m, K_{cat}/K_m and V_{max}) were calculated as previously [44].

2.7. Gene adh2 knockout

Firstly, the upstream and downstream fragments of gene *adh2* were designated as *adh2*-US and *adh2*-DS, respectively. PCR primers of *adh2*-US and *adh2*-DS were as shown in Table 1. The *adh2*-US and *adh2*-DS that adjacent to gene *adh2* were amplified by PrimerSTAR Max DNA polymerase (TaKaRa, Dalian China). PCR fragments of *adh2*-US and *adh2*-DS were purified by DNA recovery kit (TransGen, Beijing China). The purified fragments of *adh2*-US and *adh2*-DS were used as the PCR template, and *adh2*-US-F and *adh2*-DS-R were used as the primers for overlapping PCR to produce *adh2*-US-DS. The purified *adh2*-US-DS fragment and the suicide plasmid pK18*mobsacB* were digested with *Hind* III and *Xba* I at 37 °C overnight, respectively. The digested *adh2*-US-DS fragment was ligated to pK18*mobsacB* by Solution I (TaKaRa, Dalian China) at 16 °C for 1 h. The recombinant plasmid pK18*mobsacB*/*adh2*-US-DS was enriched by *E. coli* Trans1-T1.

Plasmid pK18*mobsacB*/*adh2*-US-DS was transformed into the competence cells of Δ*cp4* using the electroporation method as previous [26]. Transformed cells were coated onto nutrient agar (KmR) and incubated at 30 ℃. Single colony was transfered to 5.0 mL nutrient broth (KmR) and incubated at 180 rpm at 30 ℃. Fresh culture (200 μL) was collected by centrifugation, washed three times and reuspended in sterile nutrient broth. Serial diluted cell solutions were coated onto modified nutrient agar that contained 13 % sucrose (i.e., sucrose plate) for mutant screening. Single colony on 'sucrose plate' was selected and re-screened by nutrient agar (KmR). The colony can grow on 'sucrose plate' but susceptible to kanamycin was considered as the candidate of mutant Δ*cp4-adh2*. The mutant candidate was verified by PCR using the verify primers of ver-F and ver-R. Meawhile, the gene *adh2* knockout and mutant Δ*adh2* screening following the same procedure by using wild-type strain CW239 as the original strain.

2.8. Gene adh2 complementation

Gene *adh2* (or *cp4*) complementation to mutant Δ*cp4-adh2* followed the methods as previous [26,45]. Firstly, a complete ORF of *adh2* (or *cp4*) was amplified by PCR using the primers com-*adh2*-F/R or com-*cp4*-F/R (Table 1). PCR product of *adh2* (or *cp4*) and plasmid pSRKGm was digested by the restriction endonucleases *Nde* I and *Nhe* I at 37 °C for 10 h, respectively. The digested gene was ligated to pSRKGm by Solution I at 16 ℃ for 1 h. The recombinant plasmid pSRKGm/*adh2* (pSRKGm/*cp4*) was enriched by *E. coli* Trans1-T1 using GmR nutrient agar (50 μg/mL gentamicin). The recombinant plasmid was transformed into mutant Δ*cp4-adh2* by electroporation and screened on GmR nutrient agar [26,28]. Complementary candidates were verified by PCR using the primers as in Table 1.

2.9. Growth characterization and OTA degradation on wild-type, mutants and complementary strains

Strains CW239, Δ*adh2*, Δ*cp4-adh2*, (Δ*cp4-adh2*)/*adh2* and (Δ*p4-adh2*)/*cp4* were streaked onto nutrient agar and incubated at 30 ℃ for 3 days, respectively. The single colony was inoculated to 5.0 mL nutrient broth, and incubated at 180 rpm at 30 ℃. Until the bacterial optical density (OD_{600}) reached 0.8, the fresh culture (1.0 mL) was transferred to 100 mL nutrient broth and incubated at the same condition. Bacterial growth on each strain was examined and compared as the previous [28].

In degradation test, 1.0 mL of fresh culture of wild-type CW239, gene mutant (Δ*cp4*, Δ*adh2* or Δ*cp4-adh2*) or complementary strains [(Δ*cp4-adh2*)/*adh2* or (Δ*cp4-adh2*)/*cp4*] was transfered to 100 mL nutrient broth that contained 40 μg/L OTA, and the degradation was performed on 180 rpm at 30 ℃ for 24 h. The nutrient broth that contained 40 μg/L OTA did not inoculate any bacterial strain was set as negative control. OTA residue and the degradation product was collected, cleaned and indentified by the method of previous [24]. Herein, OTA residues were analyzed by HPLC, and OTα was identified by ultraperformance liquid chromatography-tandem mass spectrometry (UPLC-MS/MS).

2.10. Real-time quantitative PCR determination on gene adh2 expressions during OTA degradation

Gene *adh2* expressions on wild-type strain CW239, Δ*cp4*, Δ*adh2* and Δ*cp4-adh2* were determined by Real-Time quantitative PCR (RT-qPCR) at 12 h and 24 h during the OTA degradation. RNA was extracted by TransZol U Plus RNA Kit (TransGen, Beijing, China), and reverse transcription was performed by FastKing RT Kit (TIANGEN, Beijing, China) according to the manufacturers' instructions. Gene expressions were examined by RT-qPCR using Taq SYBR Green qPCR Premix (BestEnzymes, Jiangsu, China). The primer pair of F_{adh2}/R_{adh2} was used for *adh2* amplification, and the primer pair of F_{gapdh}/R_{gapdh} was used for the internal gene *gapdh* (type I glyceraldehyde-3-phosphate dehydrogenase) amplification. PCR conditions were as follows: 10 min denaturing at 95 °C, followed by 40 cycles of 10 s denaturing at 95 °C, 10 s annealing at 60 °C, 30 s extension at 72 °C.

2.11. Statistical analysis

T-test was used to data analysis in different treatments. Data are expressed as mean ± SD, $p < 0.05$ was considered as statistically significant. Statistical analysis was performed by using the GraphPad Prism Version 5 software program.

3. Results

3.1. Strain CW239 genome analysis and degradation enzymes screening

Based on OTA degradation products of OTα and L-*β*-phenylalanine by the strain CW239 in previous studies, we deduced that the enzymes responsible for amido bond hydrolysis (e.g., amidohydrolase, amidase, and carboxypeptidase) in the strain should be possible candidates for OTA degradation [27,28]. To predict the OTA hydrolases more accurate, the complete genome of *Lysobacter* sp. CW239 was sequenced and analyzed (Fig. 1, Fig. S1) and the GeneBank accession number was CP061847.1. General genomic information on strain CW239 was outlined in Table S1 -Table S3. A total of 2763 ORFs were prodicted by using the databases of ARDB, CAZyme, COG, GO, KEGG, NCBI-NR, Pfam, PHI, Swiss-Prot and VFDB (Fig. 1B). By the genome sequence analysis, a total of 15 potential hydrolases including 4 carboxypeptidases, 4 amidases and 7 amidohydrolases that related to amide bond hydrolysis were screened as the OTA degradation candidates (Table S1).

3.2. Cloning and overexpression of recombinant amidohydrolase

Two hydrolases of carboxypeptidase CP4 and amidohydrolase ADH2 were screened and validated for OTA degradation. In previous studies, we found that the carboxypeptidase CP4 showed low degradation activity to OTA, and the limited activity was also verified in this study [27,28]. In contrast, amidohydrolase ADH2 showed ultra-efficient activity to OTA degradation. As shown in Fig. 2A, a complete gene of amidohydrolase *adh2* (1317 bp) was obtained by PCR. The recombinant protein of ADH2 (rADH2) that contained a Maltose Binding Protein (MBP) tag was expressed in *E. coli* BL21 (DE3), and the *Mw* of rADH2 was about 88 kDa (Fig. 2B). After purification, almost homogeneity rADH2 was obtained and the purity was higher than 95 % (Fig. 2C).

The degradation result showed that rADH2 had ultra-efficient activity to OTA hydrolyzation (Fig. 3D). Under the 1.0 μg/mL active protein, 50 μg/L OTA was completely degraded by rADH2 in 5 min; at the same time, equivalent degraded product OTα was produced (Fig. 2E and Fig. 2F). However, the other hydrolase of rCP4 degraded only 36.8 % of OTA in 24 h under 0.5 mg/mL active protein [27,28]. The comparison result indicated that ADH2 was much more efficient than that of CP4 on OTA degradation in strain CW239. Previously, another

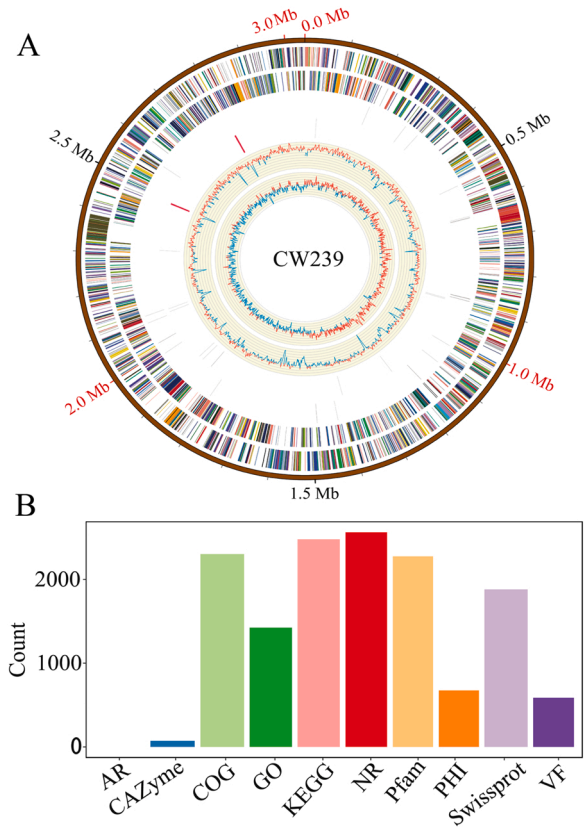

Fig. 1. The genome map and gene annotations on *Lysobacter* sp. CW239. (A) The complete genome map of strain CW239. The rings arranged from the outside to the inside as follows: 1, scale marks representing the genome; 2, protein-coding genes on forward strand; 3, protein-coding genes on reverse strand; 4, tRNA genes (black colored) and rRNA genes (red colored) on forward strand; 5, tRNA genes (black colored) and rRNA genes (red colored) on reverse strand; 6, GC content; 7, GC skew. Protein-coding genes are color coded based on their COG categories. (B) Gene annotation in various databases. The full names ofdatabaseNR, Swiss-prot, COG, KEGG, GO, CAZyme, PHI, VF and AR were specified in the section of 'materials and methods'. (For interpretation of the references to color in this figure legend, the reader is referred to the web version of this article.)

amidohydrolase ADH3 from *Stenotrophomonas acidaminiphila* CW117 can degrade 50 μg/L OTA in 2 min by 1.0 μg/mL active protein, which was significant higher than the rADH2 in this study [24]. Comprehensively, the two amidohydrolases of rADH3 and rADH2 were the most efficient OTA hydrolases among the characterized detoxify enzymes [24].

3.3. Multiple sequences alignment on OTA hydrolytic amidohydrolases

Gene *adh2* is expected to encode a protein sequence of 438 amino acids, and the theoretical pI and *Mw* were predicted to be 6.1 and 46.1 kDa, respectively. Based on the result of protein sequence alignment, the ADH2 was identified as the amidohydrolase. Protein sequence of ADH2 showed about 70 % identity to the amidohydrolases of ADH3 and Chr1_3858681_3267, but showed much lower identities to amidohydrolases of OTase (28.1 %) and *Af*OTase (12.0 %) (Fig. S2). By multiple sequences alignments, the active regions of ADH2, ADH3 and Chr1_3858681_3267 are highly conserved, and the active regions of OTase show less conservative to the amidohydrolases of ADH2, ADH3 and Chr1_3858681_3267 [17,22,24]. The active regions of *Af*OTase and NA show high identity from each other, but they show no significant identity to other amidohydrolases [25,26]. In addition, the active regions of *Bn*OTase or *Ps*SDO do not show identity to any other amidohydrolases (Fig. 3A) [19,23]. Catalytic sites analysis showed that amidohydrolases of ADH2, Chr1_3858681_3267 and OTase shared the identical catalytic amino acids to ADH3 (H_{83}, H_{85}. K_{210}, H_{251}, H_{271}, and D_{344}). Moreover, the amidohydrolases ADH3 and Chr1_3858681_3267 share the identical catalytic amino acids at the same sites [17,22,24]. However, the amino acids in putative catalytic sites of *Af*OTase (G_{98}, V_{100}, S_{226}, R_{268}, R_{288} and A_{356}) are completely different from ADH2, ADH3, Chr1_3858681_3267 and OTase, but the putative catalytic sites share 3 identical amino acids to the amidohydrolase NA from *Stenotrophomonas acidaminiphila* CW117 (Fig. 3B) [25,26]. The analysis results showed that the identified OTA hydrolytic amidohydrolases can be classified in several clades; accordingly, we designated the ADH2, ADH3, Chr1_3858681_3267 and OTase as the superfamily 1, amidohydrolases NA and *Af*OTase as superfamily 2, and designated other amidohydrolases as atypical superfamily (e.g., *Bn*OTase4, *Ps*SDO).

3.4. Enzymatic characterization of rADH2

The optimal temperature of rADH2 for OTA degradation was about 40 ℃, on which degradation ratio reached 100 %. Generally, hydrolase rADH2 showed strong adaptability to different temperatures; for example, more than 60 % enzymatic activity was retained on 20 ℃ and 60 ℃, and nearly 30 % enzymatic activity was retained on 70 ℃ (Fig. 4A). The optimal pH for rADH2 was about 7.0, and the degradation activity was strongly inhibited neither at pH 5.0 or lower nor at pH 9.0 or higher (Fig. 4B). In addition to Li^+, other metal ions all showed the negative effects on rADH2 activity at 0.01 M content; thereinto, Cu^{2+} showed the strongest inhibit rate (almost 100 %), followed by Ni^{2+}, Zn^{2+}, Mg^{2+}, Fe^{2+}, Mn^{2+} and Ca^{2+} (Fig. 4C). The rADH2 activity was significantly promoted by Li^+ at 0.05 M content or higher, and the promoting effect was positively correlated with the additive content (Fig. 4D). As shown in Fig. 4E, rADH2 activity was completely inhibited by 1 % SDS, 1.0 mg/mL proteinase K or 1.0 mg/mL proteinase K plus 1 % SDS; this result indicated that amidohydrolase rADH2 was high sensitive to protein denaturant. At the same time, the rADH2 activity could significantly be inhibited by metal-chelator of EDTA or EGTA, indicating the metal ions, especially of trace amount of Ca^{2+} might be significant to the enzymatic activity (Fig. 4F).

3.5. Kinetic constant of catalytic efficiency

Before kinetic constant characterization, ADH2 and CP4 were overexpressed in *E. coli* BL21 (DE3), and the recombinant proteins were purified by affinity chromatography (Fig. 2C and Fig. S3). The kinetic assay showed that K_m value of rADH2 was 0.00572 mM, and the K_{cat}/K_m value was 231,829.35 $s^{-1}.mM^{-1}$; while the K_m of rCP4 was 0.00168 mM, and the K_{cat}/K_m value was 0.70208 $s^{-1}.mM^{-1}$ (Table 2). The catalytic efficiency (K_{cat}/K_m) of rADH2 was about 330,203 times higher than that of rCP4; the comparison result indicated that ADH2 was the predominant OTA hydrolytic enzyme in strain CW239. The K_{cat}/K_m value of ADH2 is second only to that of ADH3 in OTA hydrolyzation, and the catalytic efficiency of ADH3 is about 1.31 times of ADH2 [24]. The K_{cat}/K_m value of ADH2 is 162,118.42 times than that of CP [46], 26, 476.33 times that of CPA, 160.47 times than that of OTase [17] and 43.23 times that of *Af*OTase [25], showing ultra-efficient OTA hydrolytic activity. By comparison of different hydrolases, we found that the catalytic efficiency of amidohydrolases (K_{cat}/K_m: 10.44 - 303,937.85 $s^{-1}.mM^{-1}$) were much higher than those of carboxypeptidases (K_{cat}/K_m: 0.00302- 8.7561 $s^{-1}.mM^{-1}$). Moreover, amidohydrolase superfamily 1 showed the highest catalytic efficiency (K_{cat}/K_m: 1444.71- 303, 937.85 $s^{-1}.mM^{-1}$), followed by superfamily 2 (K_{cat}/K_m: 10.44-5363.25 $s^{-1}.mM^{-1}$), and the atypical superfamily showed the lowest catalytic efficiency (Table 2). As the atypical superfamily, *Bn*OTase4 (protein content unkown) takes 12 h for 1 μg/mL OTA degradation [19], and *Ps*SDO takes 16 h for 5 μM OTA degradation by 15 μg active protein [23].

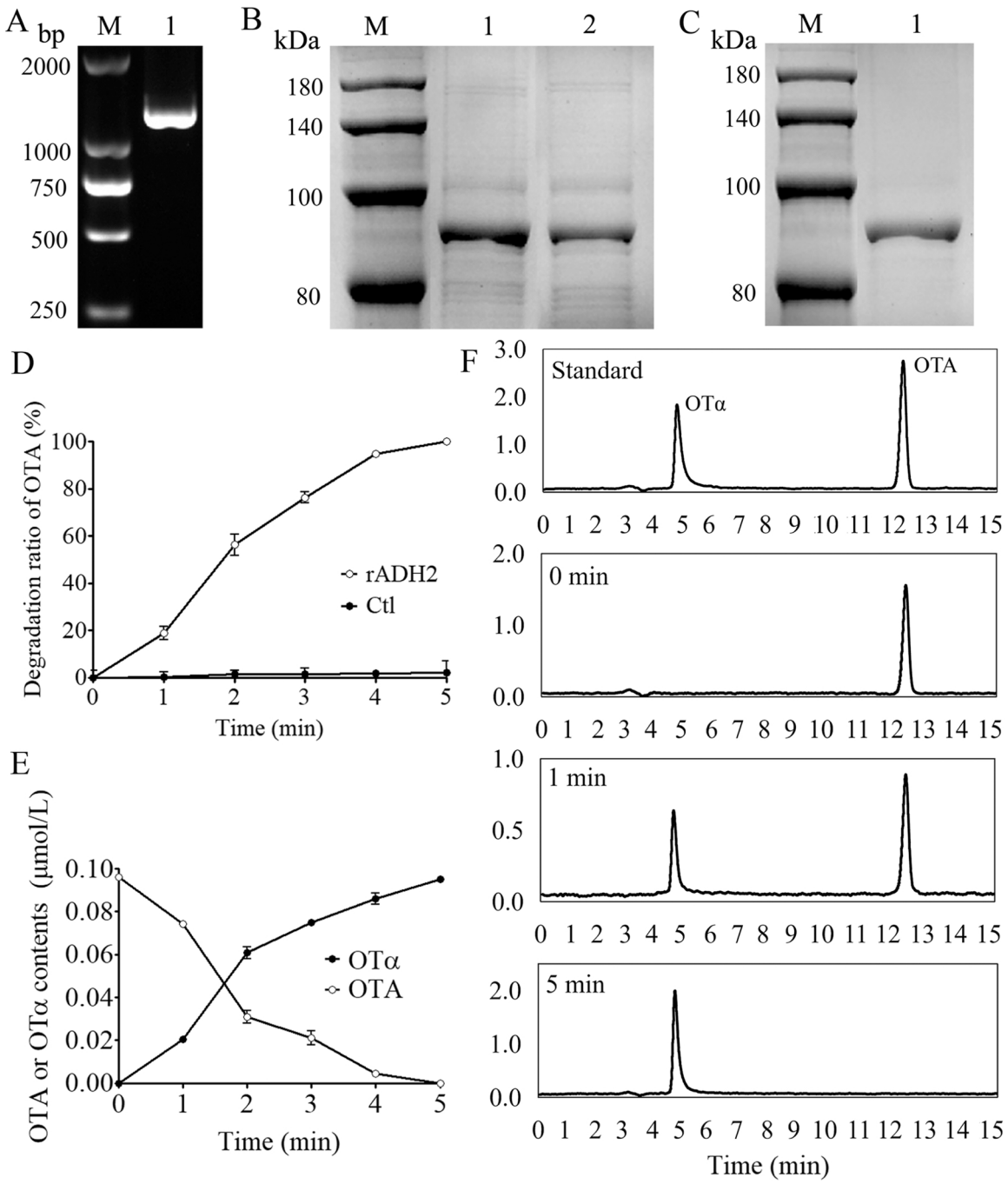

Fig. 2. Cloning, expression, protein purification and OTA degradation activity of amidohydrolase ADH2. (A) PCR verification of *adh2* on pMAL-c2X/*adh2* in *E. coli* BL21 (M, marker; lane 1, *adh2* fragment); (B) SDS-PAGE analysis of the expressed rADH2 (M, marker; lane 1, the expressed rADH2 in precipitant; lane 2, the expressed rADH2 in supernatant); (C) SDS-PAGE analysis of purified rADH2 (M, marker; lane 1, purified rADH2); (D) OTA degradation dynamic of rADH2; (E) Dynamics of OTA degradation and OTα accumulation; (F) HPLC analysis of OTA degradation by rADH2 (chromatograms from top to bottom: panel 1, OTA and OTα standards; panel 2, degradation result at 0 min; panel 3, the degradation result at 1 min; panel 4, degradation result at 5 min).

3.6. Gene knockout screening and OTA degradation verification

In this study, gene *cp4* mutant (Δ*cp4*) that constructed previously was selected as the original strain for double genes *cp4* and *adh2* mutant (Δ*cp4-adh2*) construction and screening [28]. By PCR primer pairs of *adh2*-US-F/R and *adh2*-DS-F/R, the expected fragments of *adh2*-US (477 bp) and *adh2*-DS (717 bp) was amplified (Fig. 5A). Then, the *adh2*-US and *adh2*-DS were ligated by overlapping PCR, and the PCR product of *adh2*-US-DS was 1194 bp (Fig. 5B). The recombinant plasmid pK18*mobsacB*/*adh2*-US-DS was verified by the PCR sequencing and double digestion using *Hind* III and *Xba* I (Fig. 5C and Fig. 5D). After electrotransformation and genetic recombination, the mutant Δ*cp4-adh2* was screened by KmR nutrient agar and sucrose agar, the PCR fragment on mutant Δ*cp4-adh2* was expected as 1561 bp, while the PCR fragment on original strain Δ*cp4* was 3142 bp. As shown in figures, the candidates from lane 2 were the mutant Δ*cp4-adh2* (Fig. 5E) and mutant Δ*adh2* (Fig. S4), and the PCR fragments of lane 1 were the original strain Δ*cp4* (Fig. 5E) and CW239 (Fig. S4).

Growth characteristics and OTA degradations were evaluated and compared on the wild-type CW239, single gene mutant Δ*cp4*, Δ*adh2* and

Fig. 3. Multiple sequences alignment of active regions and catalytic sites on differnent amidohydrolases. (A) Sequences alignment of active regions on amidohydrolase family proteins; (B) Catalytic sites for each amidohydrolase. Catalytic residue was highlighted in enlarged font with the specific site number. The active regions of ADH2, ADH3 and Chr1_3858681_3267 that highlighted in a dark grey are highly conserved; the active region of OTase that highlighted in light grey is less conserved to dark grey sequences. The active regions of *Af*OTase and NA that highlighted in blue show high similarity from each other, but showed no similarity to grey sequences. The active regions of *Bn*OTase and *Ps*SDO show no similarity to other amidohydrolases. The protein sequences are as follows: ADH3, QOF97534.1; *Af*OTase, OSZ37025.1; ADH2, WP_036192648.1, OTase, AIG55189.1; Chr1_3858681_3267; NA, QOF98847.1; *Bn*OTase, WLO97312.1; *Ps*SDO. WP_109614502.1. (For interpretation of the references to color in this figure legend, the reader is referred to the web version of this article.)

double genes mutant Δ*cp4-adh2*. As illustrated in Fig. 5F, the wild-type CW239 and the gene mutants (Δ*cp4*, Δ*adh2* and Δ*cp4-adh2*) showed almost the identical growth rates from each other, indicating the genes (*cp4* and *adh2*) knockout did not influence the growth characteristic of strain CW239. At 12 h incubation, the mutant Δ*cp4* degradation ratio was significantly lower than that of wild-type CW239 ($p < 0.01$); 12 h later, mutant Δ*cp4* degradation ratio was gradually recovered to wild-type CW239, and two strains showed same degradation ratio (100 %) at 24 h incubation. Although the carboxypeptidase rCP4 showed much lower activity than that of rADH2 in vitro, gene *cp4* displayed significant contribution to OTA degradation within the first 12 h in strain CW239. With incubation time extened and the ADH2 expression increased, the contribution of CP4 was not significant. In addition, the mutant Δ*adh2* almost did not show OTA degradation at 12 h, indicating very limited degradation activity of *cp4* in vivo. However, the gene *cp4* knockout (Δ*cp4*) was significantly reduced the degradation activity of the strain CW239. When the two genes *cp4* and *adh2* were successive knocked out, the double genes' mutant Δ*cp4-adh2* lost the OTA degradation activity completely (Fig. 5G). Based on degradation characters of the mutants (i.e., Δ*cp4*, Δ*adh2* and Δ*cp4-adh2*) and wild-type CW239, we comfirm that the genes *cp4* and *adh2* are the sole active agents in CW239 for OTA detoxification, but *adh2* is the predominant one.

3.7. Gene adh2 complementation and OTA degradation validation

As shown in Fig. 6A, the complete ORF of *adh2* (1317 bp) was obtained by PCR amplification. Then, the purified *adh2* fragment was digested and cloned to plasmid pSRKGm. The double digestion (*Nde* I and *Nhe* I) verified that recombinant plasmid pSRKGm/*adh2* was successfully constructed (Fig. 6B). By electrotransformation and nutrient agar screening (GmR), the complementary strain (Δ*cp4-adh2)/adh2* was obtained and verified by PCR sequencing (Fig. 6C). Meanwhile, the gene *cp4* complementary strain was successfully constructed by the same method (Fig. 6D −F).

As illustrated in Fig. 6G, wild-type CW239 and the complementary strains of (Δ*cp4-adh2)/adh2* and (Δ*cp4-adh2)/cp4* showed almost the identical growth rates, indicating the genes (*cp4* and/or *adh2*) knockout or the gene (*cp4* or *adh2*) complementation did not influence the growth characteristic of strain CW239. At 12 h incubation, the OTA degradation ratio of the complementary strain (Δ*cp4-adh2)/adh2* which only contained the gene *adh2* was significantly lower than that of *Lysobacter* sp. CW239 ($p < 0.01$) (Fig. 6H), 12 h later, the strain (Δ*cp4-adh2)/adh2* degradation ratio was gradually recovered to wild-type CW239. Wild-type CW239, complementary strain (Δ*cp4-adh2)/adh2* showed the same degradation ratio (100 %) at 24 h incubation. Meabwhile, complementary strain (Δ*cp4-adh2)/cp4* showed almost the identical degradation activity to mutant Δ*adh2* at the incubation times of 12 h and 24 h, indicating the complementary strain (Δ*cp4-adh2)/cp4* recovered the *cp4* degradation activity in vivo.

3.8. Gene adh2 expression levels in wild-type CW239 and the derived mutants

To investigate the synergistic effect of CP4 and ADH2 in strain CW239, gene *adh2* expression levels of CW239, Δ*cp4*, Δ*adh2* and Δ*cp4-adh2* were determined during the OTA degradation process. The result

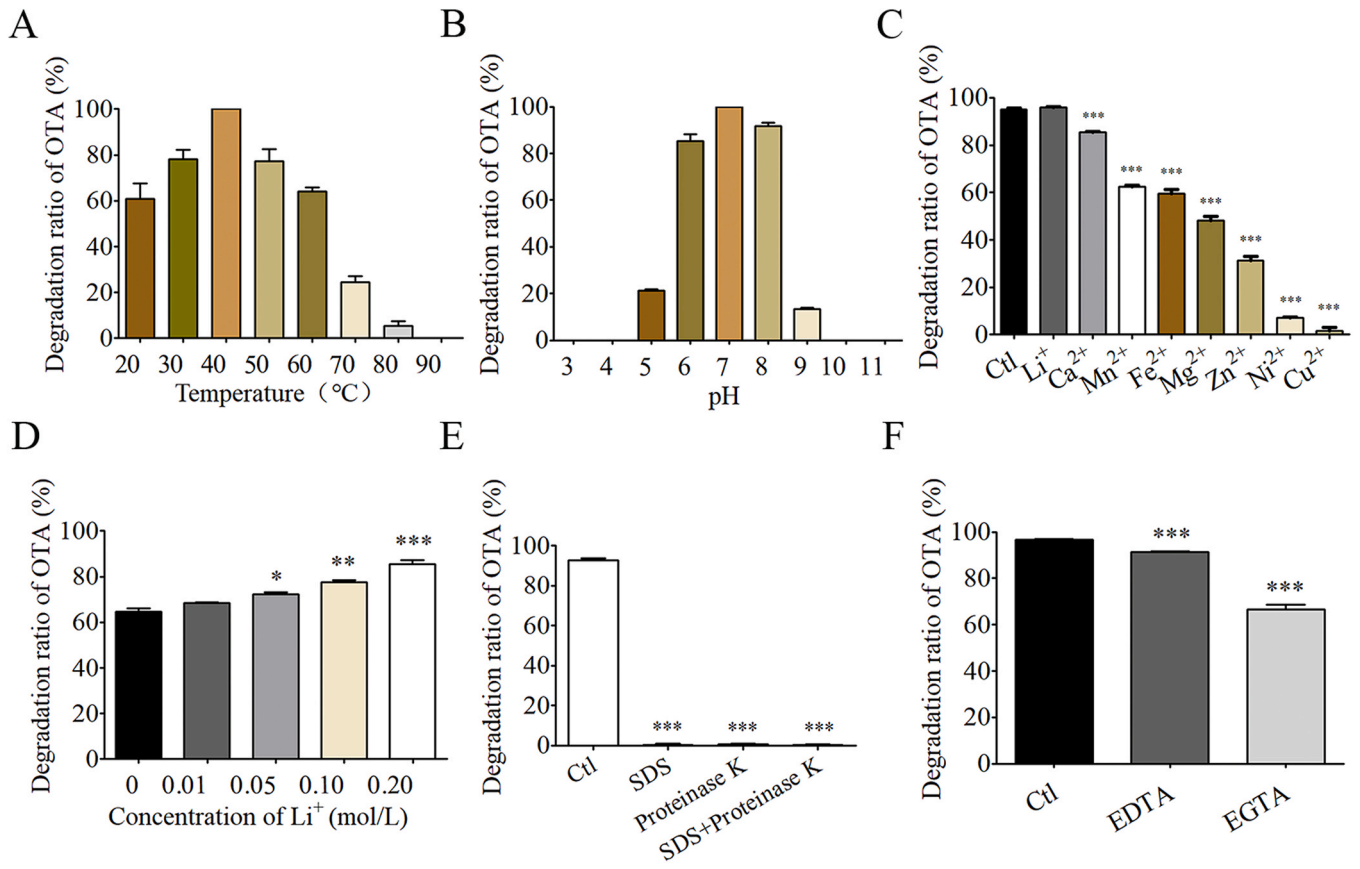

Fig. 4. Amidohydrolase rADH2 enzymatic characteristic. (A) Temperature evaluation and optimal temperature; (B) pH evaluation and optimal pH; (C) Metal ions effect on degradation activity; (D) Li^+ concentration effect on degradation activity; (E) Protein denaturant effect on degradation activity; (F) Metal-chelator effect on degradation activity.

Table 2
Kinetic constants of the OTA degradation enzymes.

Enzyme	K_m (mM)	V_{max} (mmol.min^{-1}.mg^{-1})	K_{cat} (S^{-1})	K_{cat}/K_m (s^{-1}.mM^{-1})
ADH2	0.00572	894.24	1325.12	231,829.35
CP4	0.001677	0.08007	0.00118	0.70
NA	0.0038	0.031	0.038	10.44
ADH3	0.000039	173.00	11.97	303,937.85
CPA	0.00734	0.1118	0.06428	8.7561
CPY	0.02037	0.00006	0.00006	0.00302
OTase	0.00082	1.034	1.19	1444.71
CP	0.00055	0.00074	0.00079	1.43
PJ_1540	0.00091	0.00068	0.00050	0.55
*Af*OTase	0.0025	11.19	13.24	5363.25

Kinetic constants of amidohydrolase ADH3, amidohydrolase OTase, amidohydrolase AfOTase, carboxypeptidase CPA, carboxypeptidase CPY, carboxypeptidase CP and carboxypeptidase PJ_1540 were obtained from Luo et al. [24]; kinetic constant of amidohydrolase NA was obtained from Chen et al. [26].

of RT-qPCR showed that gene *adh2* expression was not observed from Δ*adh2* and Δ*cp4-adh2*, indicating gene *adh2* was removed form the CW239. In addition, *adh2* expression levels of Δ*cp4* were lower than those of wild-type CW239, and the significant difference ($p < 0.001$) was observed on 24 h (Fig. 7). This result indicated that gene *cp4* deficiency down-regulated the expression of gene *adh2*, and thus reduced the OTA degradation activity of CW239. Due to ultra-efficient activity of ADH2, the degradation ratio of Δ*cp4* and wild-type CW239 all reached 100 % at 24 h.

4. Discussion

Mycotoxins contamination in agro-products poses serious risks on animal breeding and human health [47]. The exposure risk can be reduced or controlled by detoxification using physical, chemical and biological methods, such as microorganisms and bioenzymes. Due to the merits of environmental friendly, high efficient, and cost-effective, biodegradation (or as biotransformation) has become a promising method for mycotoxin detoxification in recent years. One of the most effective OTA detoxification method can achieve through amido bond hydrolysis by hydrolases from bacterial or fungal strains, such as *Alcaligenes faecalis*, *Brevibacterium* sp. and *Aspergillus niger*. The hydrolysis products of OTα and L-*β*-phenylalanin are recognized as nontoxic or much less toxic chemicals [17,46,48]. Two OTA hydrolases, one efficient amidohydrolase rADH2 and another less efficient carboxypeptidase CP4 were screened and characterized in *Lysobacter* sp. CW239; the two OTA hydrolases showed the same detoxification way of amido bond hydrolysis, but the activity of amidohydrolase rADH2 and carboxypeptidase CP4 varies greatly [28].

Up to now, various types of OTA detoxify enzymes (e.g., carboxypeptidase, amidohydrolase, amidase, lipase, protease A and Nudix hydrolase) have been identified and characterized. Carboxypeptidases are the earliest and widely investigated OTA detoxify enzyme from various microbial species, such as *Acinetobacter pittii*, *Lysobacter* sp., *Brevundimonas naejangsanensis* [19,27,28,49]. Amidohydrolases are the recently characterized OTA detoxify enzymes and mainly obtained from *Pseudaminobacter salicylatoxidans*, *Stenotrophomonas* sp., *Lysobacter* sp., *Aspergillus niger*, *B. naejangsanensis* and *Alcaligenes faecalis* [17,19,22–26]. Nudix hydrolase Nh-9 is another new-type OTA detoxify enzyme isolated from *Bacillus velezensis* IS-6 [20]. Luo et al. compared

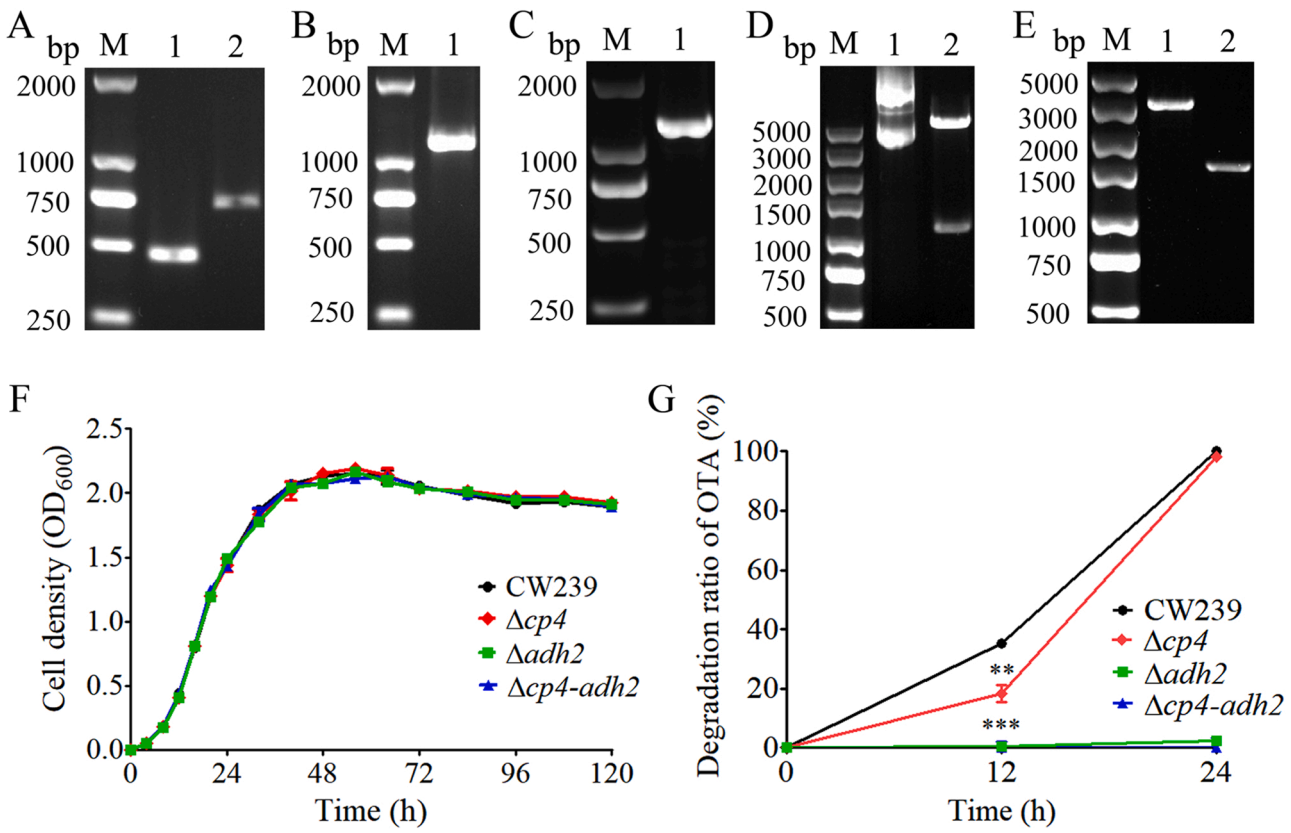

Fig. 5. Gene *adh2* mutant construction and OTA degradation verify. (A) PCR fragments of *adh2*-US and *adh2*-DS (M, DNA marker; lane 1, *adh2*-US; lane 2, *adh2*-DS); (B) overlap PCR fragment of *adh2*-US-DS (M, DNA marker; lane 1, *adh2*-US-DS); (C) PCR verification of *adh2*-US-DS on pK18*mobsacB/adh2*-US-DS (M, DNA marker; lane 1, *adh2*-US-DS fragment); (D) plasmid pK18*mobsacB/adh2*-US-DS digestion by Xba I and Hind III (M, DNA marker; lane 1, circular pK18*mobsacB/adh2*-US-DS; lane 2, digested pK18*mobsacB/adh2*-US-DS); (E) PCR verification on gene *adh2* mutant (M, DNA Marker; lane 1, mutant Δ*cp4*; lane 2, mutant Δ*cp4-adh2*); (F) the growth dynamics of CW239, Δ*cp4*, Δ*adh2* and Δ*cp4-adh2*; (G) the OTA degradation dynamics of CW239, Δ*cp4*, Δ*adh2* and Δ*cp4-adh2*.

the enzymatic activity of different types of detoxify enzymes, and the amidohydrolase ADH3 activity was much higher than those of carboxypeptidases and other identified OTA hydrolase [24]. Since OTase (previously named as amidase) was characterized by Dobritzsch et al. in 2014, several amidohydrolases have been characterized in recent years [17]; meanwhile, some other enzymes, (e.g., salicylate 1,2-dioxygenase *Ps*SDO) were also characterized as the amidohydrolase [23].

Based on the analysis result of active region and catalytic sites in this study, the amidohydrolases were classified into superfamily 1 (e.g., ADH2, ADH3, Chr1_3858681_3267 and OTase), superfamily 2 (e.g., NA and *Af*OTase) and atypical superfamily (e.g., *Bn*OTase, *Ps*SDO). Interestingly, the catalytic efficiency of each amidohydrolase superfamily is quite different (Table 2). Superfamily 1 showed the highest catalytic efficiency, especially of ADH3 (K_{cat}/K_m: 303,937.85 $s^{-1}.mM^{-1}$) and ADH2 (K_{cat}/K_m: 231,829.35 $s^{-1}.mM^{-1}$). Superfamily 2 was the less efficient amidohydrolase next to superfamily 1. The K_{cat}/K_m value of *Af*OTase reached 5363.25 $s^{-1}.mM^{-1}$ and the K_{cat}/K_m value of NA was 10.4 $s^{-1}.mM^{-1}$ [26]. In contrast, the catalytic efficiency of atypical superfamily (e.g., *Bn*OTase, *Ps*SDO) was much lower than those of superfamily 1 and superfamily 2. Although the K_{cat}/K_m values of *Bn*OTase and *Ps*SDO were not determined (or not detailed) in the original literatrues, the two amidohydrolases needed more than 10 h to complete the degradation process, we supposed that the catalytic efficiencies might be similar to those of carboxypeptidases [19,23]. Generally, amidohydrolases especially of superfamily 1 are the most efficient type among the OTA detoxify enzymes, followed by Nudix hydrolase and carboxypeptidases.

With biodetoxification study development, a variety of OTA degradation microbial strains and enzymes have been obtained. Microbial strain can degrade OTA by single gene (e.g., *A. niger* UVK143 and *P. salicylatoxidans* DSM 6986 ^{T}), and can also degrade OTA by multiple genes in one strain (e.g., *Stenotrophomonas* sp. CW117, *Lysobacter* sp. CW239, *B. naejangsanensis* ML17) [19]. Two amidohydrolases of ADH3 and NA were obtained in *Stenotrophomonas* sp. CW117, and the combined effect was observed on OTA degradation [26]. Four type hydrolases of peptidase (*Bn*OTAase1), carboxypeptidase (*Bn*OTAase2), metallopeptidase (*Bn*OTAase3) and amidohydrolase (*Bn*OTAase3) were characterized for OTA degradation in the *B. naejangsanensis* ML17, but the combined effect was unkown [19]. In this study, two types of hydrolases carboxypeptidase CP4 and amidohydrolase ADH2 were indentified, and the catalytic efficiency of rADH2 was about 330,203 times higher than that of rCP4. Although the activity of rCP4 was almost negligible compared to that of rADH2 in vitro, gene *cp4* displayed significant contributions to OTA degradation within the first 12 h in strain CW239. Hence, the carboxypeptidase and amidohydrolase showed the synergistic effect on OTA degradation in *Lysobacter* sp. CW239. For biodetoxification applications, some studies show that mycotoxins degradation strains from animal gut environments might be used as the probiotics for farm animals, and gut microbial strains are considered as an efficetive way for detoxification applications [50]. However, the strain CW239 in this study was isolated from soil sample, and the colonization characters in animal gut and its toxicological effects on animals are unknown; thus, the ADH2 zymin might be a potential way of industrial application. Before detoxify enzyme ADH2 application, further studies of protein yields from the heterologous expression systems, the environmental tolerance of foods or feedstuffs, and the cost of production should be carefully evaluated.

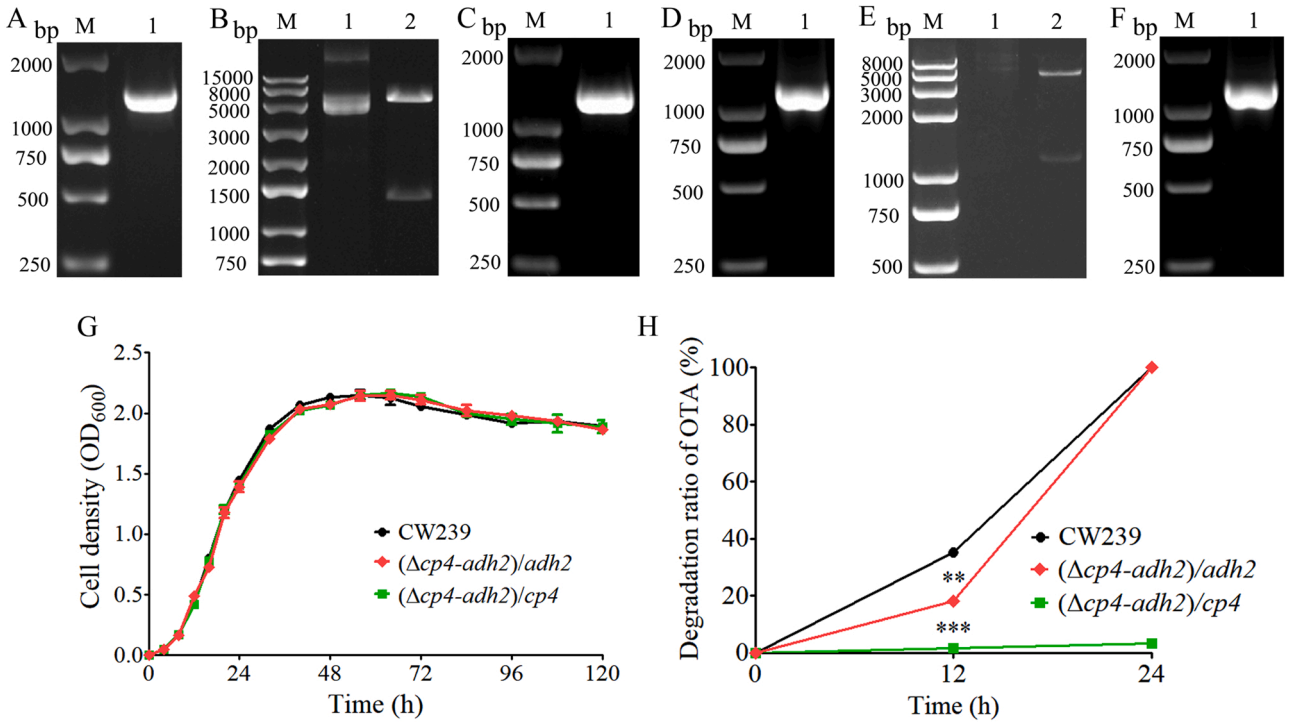

Fig. 6. Gene complementary strains construction and OTA degradation verify. (A) PCR product of gene *adh2* (M, DNA marker; lane 1, *adh2* fragment); (B) plasmid pSRK-Gm/*adh2* digestion by *Nde* I and *Nhe* I (M, DNA marker; lane 1, circular pSRK-Gm/*adh2*; lane 2, digested pSRK-Gm/*adh2*); (C) PCR verify on gene *adh2* complementary strain (M, DNA Marker; lane 1, strain (Δ*cp4-adh2*)/*adh2*); (D) PCR product of gene *cp4* (M, DNA marker; lane 1, *cp4* fragment); (E) plasmid pSRK-Gm/*cp4* digestion by *Nde* I and *Nhe* I (M, DNA marker; lane 1, circular pSRK-Gm/*cp4*; lane 2, digested pSRK-Gm/*cp4*); (F) PCR verify on gene *cp4* complementary strain (M, DNA Marker; lane 1, strain (Δ*cp4-adh2*)/*cp4*); (G) the growth dynamics for CW239, (Δ*cp4-adh2*)/*adh2* and (Δ*cp4-adh2*)/*cp4*; (E) the OTA degradation dynamics of CW239, (Δ*cp4-adh2*)/*adh2* and (Δ*cp4-adh2*)/*cp4*.

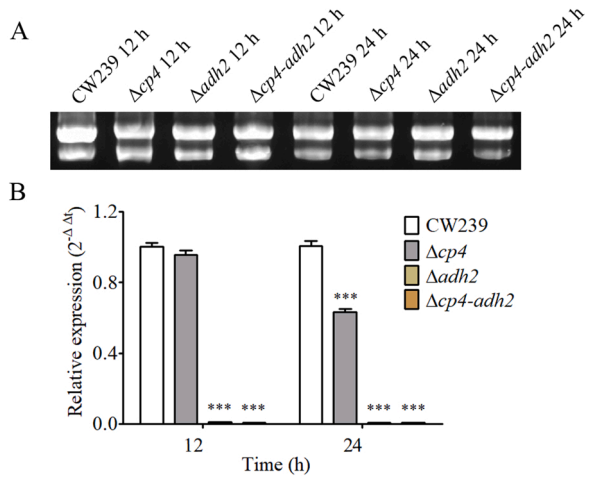

Fig. 7. Gene *adh2* expression levels in wild-type CW239 and the derived gene mutants during OTA degradation. (A) RNAs extracted from wild-type CW239 and the mutants of Δ*cp4*, Δ*adh2* and Δ*cp4-adh2*; (B) gene *adh2* expression levels in wild-type CW239 and the mutants of Δ*cp4*, Δ*adh2* and Δ*cp4-adh2* by RT-qPCR (Student's T test, ***, $p < 0.001$, refers to mutant strain versus CW239; $n = 9$).

5. Conclusion

Other than carboxypeptidase CP4, another amidohydrolase ADH2 was screened for OTA hydrolysis from the degradation strain CW239 by genomic analysis. The amidohydrolase ADH2 showed ultra-efficient hydrolytic activity on OTA that can completely degrade 50 μg/L OTA within only 5 min. Meanwhile, the two hydrolases (i.e., carboxypeptidase CP4 and amidohydrolase ADH2) are sole agents in strain CW239 for OTA degradation. Other than genes *cp4* and *adh2*, no other degradation gene existed in the strain CW239. Although the two OTA detoxify enzymes of CP4 and ADH2 were different types of hydrolases, they showed the same detoxification manner and all transformed OTA to ochratoxin α (OTα) and L-*β*-phenylalanine. During the OTA degradation, the ADH2 was the overwhelming efficient catalyst, but the gene *cp4* could regulate the expression level of gene *adh2* in the strain CW239, and the two hydrolases co-degraded OTA in CW239 by synergistic effect. In shortly, results of this study are highly significant to OTA detoxification and the contamination controls during agro-products production.

Environmental implications

Ochratoxin A (OTA) is a toxic secondary metabolite that widely contaminates agricultural production environment and agro-products. OTA degradation methods showed high interest in contamination control in food production. Previously, a carboxypeptidase CP4 had been characterized for OTA degradation in the efficient strain *Lysobacter* sp. CW239. Here, another ultra-efficient amidohydrolase ADH2 was further screened for OTA hydrolysis in CW239. The OTA combined degradation actions of the two hydrolases in CW239 were investigated by in vitro and in vivo methods. The degradation mechanism the CW239 and the ultra-efficient detoxify enzyme ADH2 would enable the applications in agricultural productions and food safety.

CRediT authorship contribution statement

Na Li: Methodology, Investigation, Data curation. **Yu Zhou:** Writing – review & editing, Supervision, Funding acquisition, Conceptualization. **Liang Zhang:** Writing – review & editing, Methodology, Data

curation. **Xiaojie Fu:** Writing – original draft, Methodology, Investigation, Data curation. **Xuanjun Zhang:** Methodology, Investigation, Formal analysis. **Qingru Fei:** Methodology, Investigation, Formal analysis, Data curation.

Declaration of Competing Interest

The authors declare that they have no known competing financial interests or personal relationships that could have appeared to influence the work reported in this paper.

Data availability

Data will be made available on request.

Acknowledgement

This study was supported by the National Natural Science Foundation of China (32172319; U22A20442) and Research Funds of Joint Research Center for Food Nutrition and Health of IHM (2023SJY02).

Appendix A. Supporting information

Supplementary data associated with this article can be found in the online version at doi:10.1016/j.jhazmat.2024.134716.

References

[1] Wang, L., Hua, X., Shi, J., Jing, N., Ji, T., Lv, B., et al., 2022. Ochratoxin A: occurrence and recent advances in detoxification. Toxicon 210, 11–18. https://doi.org/10.1016/j.toxicon.2022.02.010.
[2] Kumar, P., Mahato, D.K., Sharma, B., Borah, R., Haque, S., Mahmud, M.M.C., et al., 2020. Ochratoxins in food and feed: occurrence and its impact on human health and management strategies. Toxicon 187, 151–162. https://doi.org/10.1016/j.toxicon.2020.08.031.
[3] Ülger, T.G., Uçar, A., Çakıroğlu, F.P., Yilmaz, S., 2020. Genotoxic effects of mycotoxins. Toxicon 185, 104–113. https://doi.org/10.1016/j.toxicon.2020.07.004.
[4] Santos, A.R., Carreiró, F., Freitas, A., Barros, S., Brites, C., Ramos, F., et al., 2022. Mycotoxins contamination in rice: analytical methods, occurrence and detoxification strategies. Toxins 14 (9), 647. https://doi.org/10.3390/toxins14090647.
[5] Perrone, G., Gallo, A., 2017. *Aspergillus* species and their associated mycotoxins. Methods Mol Biol 1542 33–49. https://doi.org/10.1007/978-1-4939-6707-0_3.
[6] Pleadin, J., Frece, J., Markov, K., 2019. Mycotoxins in food and feed. Adv Food Nutr Res 89, 297–345. https://doi.org/10.1016/bs.afnr.2019.02.007.
[7] Shanakhat, H., Sorrentino, A., Raiola, A., Romano, A., Masi, P., Cavella, S., 2018. Current methods for mycotoxins analysis and innovative strategies for their reduction in cereals: an overview. J Sci Food Agric 98 (11), 4003–4013. https://doi.org/10.1002/jsfa.8933.
[8] Chen, W., Li, C., Zhang, B., Zhou, Z., Shen, Y., Liao, X., et al., 2018. Advances in biodetoxification of ochratoxin A-a review of the past five decades. Front Microbiol 9, 1386. https://doi.org/10.3389/fmicb.2018.01386.
[9] Zhu, Y., Hassan, Y.I., Lepp, D., Shao, S., Zhou, T., 2017. Strategies and methodologies for developing microbial detoxification systems to mitigate mycotoxins. Toxins 9 (4), 130. https://doi.org/10.3390/toxins9040130.
[10] Abraham, N., Chan, E.T.S., Zhou, T., Seah, S.Y.K., 2022. Microbial detoxification of mycotoxins in food. Front Microbiol 13, 957148. https://doi.org/10.3389/fmicb.2022.957148.
[11] Muhialdin, B.J., Saari, N., Meor Hussin, A.S., 2020. Review on the biological detoxification of mycotoxins using lactic acid bacteria to enhance the sustainability of foods supply. Molecules 25 (11), 2655. https://doi.org/10.3390/molecules25112655.
[12] Shang, L., Bai, X., Chen, C., Liu, L., Li, M., Xia, X., et al., 2019. Isolation and identification of a *Bacillus megaterium* strain with ochratoxin A removal ability and antifungal activity. Food Control 106, 106743. https://doi.org/10.1016/j.foodcont.2019.106743.
[13] Azam, M.S., Yu, D., Liu, N., Wu, A., 2019. Degrading ochratoxin A and zearalenone mycotoxins using a multifunctional recombinant enzyme. Toxins 11 (5), 301. https://doi.org/10.3390/toxins11050301.
[14] Llobregat, B., González-Candelas, L., Ballester, A.R., 2022. Ochratoxin A defective *Aspergillus carbonarius* mutants as potential biocontrol agents. Toxins 14 (11), 745. https://doi.org/10.3390/toxins14110745.
[15] Zhang, X., Yang, H., Apaliya, M.T., Zhao, L., Gu, X., Zheng, X., et al., 2018. The mechanisms involved in ochratoxin A elimination by *Yarrowia lipolytica* Y-2. Ann Appl Biol 173, 164–174. https://doi.org/10.1111/aab.12452.
[16] Cho, S.M., Jeong, S.E., Lee, K.R., Sudhani, H.P., Kim, M., Hong, S.Y., et al., 2016. Biodegradation of ochratoxin A by *Aspergillus tubingensis* isolated from Meju. J Microbiol Biotechnol 26 (10), 1687–1695. https://doi.org/10.4014/jmb.1606.06016.
[17] Dobritzsch, D., Wang, H., Schneider, G., Yu, S., 2014. Structural and functional characterization of ochratoxinase, a novel mycotoxin-degrading enzyme. Biochem J 462 (3), 441–452. https://doi.org/10.1042/BJ20140382.
[18] de Oliveira Garcia, S., Sibaja, K.V.M., Nogueira, W.V., Feltrin, A.C.P., Pinheiro, D. F.A., Cerqueira, M.B.R., et al., 2020. Peroxidase as a simultaneous degradation agent of ochratoxin A and zearalenone applied to model solution and beer. Food Res Int 131, 109039. https://doi.org/10.1016/j.foodres.2020.109039.
[19] Peng, M., Zhang, Z., Xu, X., Zhang, H., Zhao, Z., Liang, Z., 2023. Purification and characterization of the enzymes from *Brevundimonas naejangsanensis* that degrade ochratoxin A and B. Food Chem 419, 135926. https://doi.org/10.1016/j.foodchem.2023.135926.
[20] Jahan, I., Tai, B., Ma, J., Hussain, S., Du, H., Guo, L., et al., 2023. Identification of a novel *Bacillus velezensis* IS-6 nudix hydrolase Nh-9 involved in ochratoxin A detoxification by transcriptomic profiling and functional verification. J Agric Food Chem 71 (26), 10155–10168. https://doi.org/10.1021/acs.jafc.3c01910.
[21] Adegoke, T.V., Yang, B., Xing, F., Tian, X., Wang, G., Tai, B., et al., 2023. Microbial enzymes involved in the biotransformation of major mycotoxins. J Agric Food Chem 71 (1), 35–51. https://doi.org/10.1021/acs.jafc.2c06195.
[22] Gonaus, C., Wieland, L., Thallinger, G.G., Prasad, S., 2023. Ochratoxin A degrading enzymes of *Stenotrophomonas* sp. 043-1a. FEMS Microbiol Lett 370, fnad028. https://doi.org/10.1093/femsle/fnad028.
[23] Sánchez-Arroyo, A., Plaza-Vinuesa, L., Rivas, B.L., Mancheño, J.M., Muñoz, R., 2023. The salicylate 1,2-dioxygenase from *Pseudaminobacter salicylatoxidans* DSM 6986T is a bifunctional enzyme that inactivates the mycotoxin ochratoxin A by a novel amidohydrolase activity. Int J Biol Macromol 237, 124230. https://doi.org/10.1016/j.ijbiomac.2023.124230.
[24] Luo, H., Wang, G., Chen, N., Fang, Z., Xiao, Y., Zhang, M., et al., 2022. A superefficient ochratoxin A hydrolase with promising potential for industrial applications. Appl Environ Microbiol 88 (2), e0196421. https://doi.org/10.1128/AEM.01964-21.
[25] Zhang, H., Zhang, Y., Yin, T., Wang, J., Zhang, X., 2019. Heterologous expression and characterization of a novel ochratoxin A degrading enzyme, N-acyl-L-amino acid amidohydrolase, from *Alcaligenes faecalis*. Toxins 11 (9), 518. https://doi.org/10.3390/toxins11090518.
[26] Chen, N., Fei, Q., Luo, H., Fang, Z., Xiao, Y., Du, Z., et al., 2022. Isoenzyme N-acyl-L-amino acid amidohydrolase NA increases ochratoxin A degradation efficacy of *Stenotrophomonas* sp. CW117 by enhancing amidohydrolase ADH3 stability. Microbiol Spectr 10 (4), e0220522. https://doi.org/10.1128/spectrum.02205-22.
[27] Wei, W., Qian, Y., Wu, Y., Chen, Y., Peng, C., Luo, M., et al., 2020. Detoxification of ochratoxin A by *Lysobacter* sp. CW239 and characteristics of a novel degrading gene carboxypeptidase *cp4*. Environ Pollut 258, 113677. https://doi.org/10.1016/j.envpol.2019.113677.
[28] Qian, Y., Zhang, X., Fei, Q., Zhou, Y., 2021. Comments on the ochratoxin A degradation mechanism by *Lysobacter* sp. CW239 - Wei Wei et al. (2020). Environ Pollut 281, 117063. https://doi.org/10.1016/j.envpol.2021.117063.
[29] Hyatt, D., Chen, G.L., Locascio, P.F., Land, M.L., Larimer, F.W., Hauser, L.J., 2010. Prodigal: prokaryotic gene recognition and translation initiation site identification. BMC Bioinforma 11, 119. https://doi.org/10.1186/1471-2105-11-119.
[30] Delcher, A.L., Bratke, K.A., Powers, E.C., Salzberg, S.L., 2007. Identifying bacterial genes and endosymbiont DNA with Glimmer. Bioinformatics 23 (6), 673–679. https://doi.org/10.1093/bioinformatics/btm009.
[31] Galperin, M.Y., Kristensen, D.M., Makarova, K.S., Wolf, Y.I., Koonin, E.V., 2019. Microbial genome analysis: the COG approach. Brief Bioinform 20 (4), 1063–1070. https://doi.org/10.1093/bib/bbx117.
[32] O'Leary, N.A., Wright, M.W., Brister, J.R., Ciufo, S., Haddad, D., McVeigh, R., et al., 2016. Reference sequence (RefSeq) database at NCBI: current status, taxonomic expansion, and functional annotation. Nucleic Acids Res 44 (D1), D733–D745. https://doi.org/10.1093/nar/gkv1189.
[33] The Gene Ontology Consortium, 2019. The Gene Ontology Resource: 20 years and still GOing strong. Nucleic Acids Res 47 (D1), D330–D338. https://doi.org/10.1093/nar/gky1055.
[34] Kanehisa, M., Furumichi, M., Tanabe, M., Sato, Y., Morishima, K., 2017. KEGG: new perspectives on genomes, pathways, diseases and drugs. Nucleic Acids Res 45 (D1), D353–D361. https://doi.org/10.1093/nar/gkw1092.
[35] Mistry, J., Chuguransky, S., Williams, L., Qureshi, M., Salazar, G.A., Sonnhammer, E.L.L., et al., 2021. Pfam: the protein families database in 2021. Nucleic Acids Res 49 (D1), D412–D419. https://doi.org/10.1093/nar/gkaa913.
[36] Boutet, E., Lieberherr, D., Tognolli, M., Schneider, M., Bansal, P., Bridge, A.J., et al., 2016. UniProtKB/Swiss-Prot, the manually annotated section of the UniProt Knowledgebase: how to use the entry view. Methods Mol Biol 1374, 23–54. https://doi.org/10.1007/978-1-4939-3167-5_2.
[37] Drula, E., Garron, M.L., Dogan, S., Lombard, V., Henrissat, B., Terrapon, N., 2022. The carbohydrate-active enzyme database: functions and literature. Nucleic Acids Res 50 (D1), D571–D577. https://doi.org/10.1093/nar/gkab1045.
[38] Urban, M., Cuzick, A., Seager, J., Wood, V., Rutherford, K., Venkatesh, S.Y., et al., 2020. PHI-base: the pathogen-host interactions database. Nucleic Acids Res 48 (D1), D613-D620. https://doi.org/10.1093/nar/gkz904.
[39] Liu, B., Zheng, D., Zhou, S., Chen, L., Yang, J., 2022. VFDB 2022: a general classification scheme for bacterial virulence factors. Nucleic Acids Res 50 (D1), D912–D917. https://doi.org/10.1093/nar/gkab1107.
[40] Liu, B., Pop, M., 2009. ARDB–antibiotic resistance genes database. Nucleic Acids Res 37, D443–D447. https://doi.org/10.1093/nar/gkn656.

[41] Pace, C.N., Vajdos, F., Fee, L., Grimsley, G., Gray, T., 1995. How to measure and predict the molar absorption coefficient of a protein. Protein Sci 4 (11), 2411–2423. https://doi.org/10.1002/pro.5560041120.
[42] Teufel, F., Almagro Armenteros, J.J., Johansen, A.R., Gíslason, M.H., Pihl, S.I., Tsirigos, K.D., et al., 2022. SignalP 6.0 predicts all five types of signal peptides using protein language models. Nat Biotechnol 40 (7), 1023–1025. https://doi.org/10.1038/s41587-021-01156-3.
[43] Artimo, P., Jonnalagedda, M., Arnold, K., Baratin, D., Csardi, G., de Castro, E., et al., 2012. ExPASy: SIB bioinformatics resource portal. Nucleic Acids Res 40, W597–W603. https://doi.org/10.1093/nar/gks400.
[44] Stander, M.A., Bornscheuer, U.T., Henke, E., Steyn, P.S., 2000. Screening of commercial hydrolases for the degradation of ochratoxin A. J Agric Food Chem 48 (11), 5736–5739. https://doi.org/10.1021/jf000413j.
[45] Khan, S.R., Gaines, J., Roop, R.M., Farrand, S.K., 2008. Broad-host-range expression vectors with tightly regulated promoters and their use to examine the influence of TraR and TraM expression on Ti plasmid quorum sensing. Appl Environ Microbiol 74 (16), 5053–5062. https://doi.org/10.1128/AEM.01098-08.
[46] Chang, X., Wu, Z., Wu, S., Dai, Y., Sun, C., 2015. Degradation of ochratoxin A by *Bacillus amyloliquefaciens* ASAG1. Food Addit Contam Part A Chem Anal Control Expo Risk Assess 32 (4), 564–571. https://doi.org/10.1080/19440049.2014.991948.
[47] Ostry, V., Malir, F., Toman, J., Grosse, Y., 2017. Mycotoxins as human carcinogens-the IARC Monographs classification. Mycotoxin Res 33 (1), 65–73. https://doi.org/10.1007/s12550-016-0265-7.
[48] Mwabulili, F., Xie, Y., Li, Q., Sun, S., Yang, Y., Ma, W., 2023. Research progress of ochratoxin a bio-detoxification. Toxicon 222, 107005. https://doi.org/10.1016/j.toxicon.2022.107005.
[49] Yang, Y., Zhong, W., Wang, Y., Yue, Z., Zhang, C., Sun, M., et al., 2024. Isolation, identification, degradation mechanism and exploration of active enzymes in the ochratoxin A degrading strain *Acinetobacter pittii* AP19. J Hazard Mater 465, 133351. https://doi.org/10.1016/j.jhazmat.2023.133351.
[50] Sun, Y., Jiang, J., Mu, P., Lin, R., Wen, J., Deng, Y., 2022. Toxicokinetics and metabolism of deoxynivalenol in animals and humans. Arch Toxicol 96, 2639–2654. https://doi.org/10.1007/s00204-022-03337-8.